Numerical Evaluation of the Pseudo-Tridents Production Cross-Section

by **C. Piron, M. Gailloud, Ph. Rosselet** and **M. Biasutti**

(Laboratoire de Recherches Nucléaires, E.P.U.L., Lausanne)

Summary. The number of apparent tridents produced by Bremsstrahlung has been calculated for arbitrary experimental conditions and $E/mc^2 < 10^5$.

I. Introduction

Several authors have studied the direct production of electron pairs by charged particles in photographic emulsions and more recently in diffusion chambers. It is well known that, due to the finite resolution of the detector, pairs produced by conversion of Bremsstrahlung photons on the track of the primary particle are indistinguishable from direct pairs. The number of these spurious events (pseudo-tridents) can be evaluated in a semi empirical way from the number of pairs observed within a given distance to the track[1-3]. This procedure implies the knowledge of the theoretical distribution of the pairs, and of the scanning efficiency as a function of the distance to the primary track; it is therefore subject to a serious experimental bias. In this work, the number of pseudo-tridents per unit length has been calculated in a completely theoretical way from the known radiation and materialization cross-sections, using the spatial distribution function of multiple Coulomb scattering given by Rossi[4].

2. Derivation of the general formula for the number of pseudo-tridents

Let us consider a particle of charge e, mass m and energy E moving in a given medium. Let n_f be the number of Bremsstrahlung pairs produced per unit length inside a tube of radius ϱ around the trajectory. n_f is a constant at sufficiently large distances from the boundaries of the medium, that is as soon as the mean square lateral displacement σ due to the multiple Coulomb scattering is larger than ϱ[5] *). We have then:

$$n_f = \int_{2 m_e c^2}^{E} \sum_b (k)dk \int_l \int_0 \sum_b (E, k, \theta,)dl \int\int_{C(l\theta, \varrho)} dy\, dz \frac{1}{\pi} \frac{1}{\sigma^2} e^{-\frac{y^2+z^2}{\sigma^2}} d\theta \quad (1)$$

where $$\sum_b (E, k, \theta)\, dk\, d\theta$$

---

*) This can be seen in Figure 5 of reference [5] for a particular case.

is the macroscopic radiation cross-section, differential in photon energy k and emission angle θ. θ is the angle between the emitted photon and the outgoing particle.

$\sum_p(k)$ is the total macroscopic cross-section for the conversion of a photon of energy k.

$$\sigma^2 = \frac{D^2 \cdot l^3}{X_0 \, (E-k)^2}$$

X_0 is the radiation length of the medium; D is a constant ($3\,D^2 = E_s^2$ as in equation (7) page 68 of reference [4]).

The notation $C(l\theta, \varrho)$ means that the integration with respect to y and z is carried out in a circle of radius ϱ centered at a distance $l\,\theta$ from the tangent to the trajectory (Fig. 1).
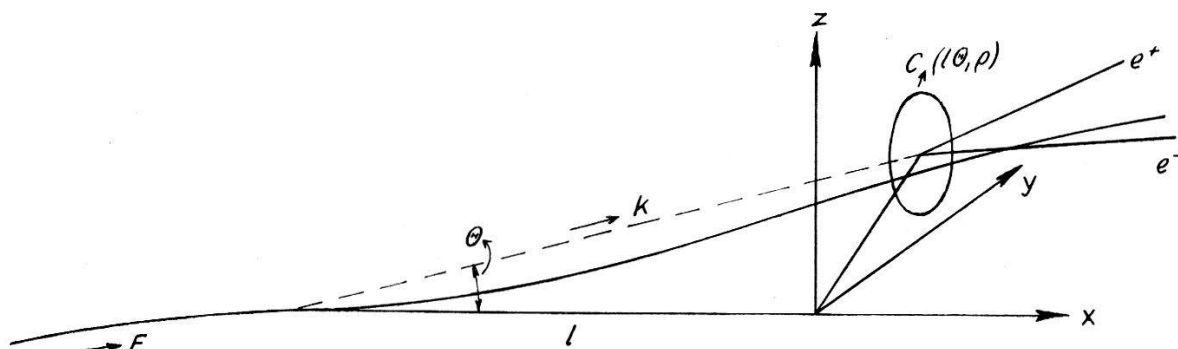

Fig. 1

For useful values of ϱ, the average distance between the emission and the conversion of a photon is small compared to X_0, as will be verified later on. We have therefore neglected, in equation (1), the energy loss of the particle over the distance l.

The angular distribution of the radiated photons is given by a hardly workable expression which can be written, with a good approximation, as a function of $\theta_0 \, E/mc^2$ where θ_0 is the angle between the initial particle and the photon [6]. The symmetry under time reversal allows us to write it as a function of $\tau = \theta \, (E - k)/mc^2$:

$$\sum_b (E, k, \theta) \, d\theta \cong \sum_b (E, k) \, dn \left(\frac{\theta \, (E-k)}{mc^2} \right)$$

where dn is the fraction of the photons of energy k emitted in the elementary solid angle $2\,\pi \sin\theta \, d\theta$ and

$$\sum_b (E, k) = \left(\frac{m_e}{m} \right)^2 \frac{1}{X_0} \frac{dk}{k} . \tag{2}$$

Substituting in equation (1) we get

$$n_f = \int_k \sum_p (k) \, dk \cdot \sum_b (E, k) \cdot \bar{l} \, (E - k, \varrho, m, X_0, D^2) \tag{3}$$

with

$$\bar{l} = \int_l dl \int_\theta dn \left(\frac{\theta \, (E-k)}{mc^2} \right) \iint_{C(l\theta, \varrho)} dy \, dz \, \frac{1}{\pi} \, \frac{X_0 \, (E-k)^2}{D^2 \cdot l^3} \cdot e^{-\frac{(y^2 + z^2) \, X_0 \, (E-k)^2}{D^2 \, l^3}} \tag{4}$$

3. Computation of $\bar{l}$

$\bar{l}$ is the average path length of the photons converted inside the tube of radius ϱ. $\bar{l}$ depends on many parameters, but we can substitute for it a function depending explicitly on one variable only. Defining:

$$g = l \frac{D^2}{(mc^2)^2} \frac{1}{X_0} \quad , \quad \bar{g} = \bar{l} \frac{D^2}{(mc^2)^2} \frac{1}{X_0}$$

$$r'_y = y \frac{(E-k) D^2}{(mc^2)^3 X_0} \quad , \quad r'_z = z \frac{(E-k) D^2}{(mc^2)^3 X_0} \quad , \quad r = \varrho \frac{(E-k) D^2}{(mc^2)^3 X_0} \tag{5}$$

and noting that

$$\frac{(y^2 + z^2) X_0 (E-k)^2}{D^2 l^3} = \frac{r'^2}{g^3}$$

and

$$\frac{l\theta (E-k) D^2}{(mc^2)^3 \cdot X_0} = g\tau$$

equation (4) becomes

$$\bar{g} = \int_g dg \int_\tau dn(\tau) \iint_{C(g\tau, r)} dr'_y \, dr'_z \frac{1}{\pi} \frac{1}{g^3} e^{-\frac{r'^2}{g^3}} \tag{6}$$

The dimensionless function $\bar{g}$ is independent of the medium, the mass and the energy of the particle, but depends only on the parameter r.

For the actual computation of $\bar{g}(r)$, we took for $dn(\tau)$ the values calculated by KOCH and MOTZ[6] for 300 MeV electrons and for $k/E = 0{,}3$ (based on the Schiff differential cross-section). These values were then normalized to unity.

The numerical integrations were performed on the Zebra electronic computer of the E. P. U. L.*). To simplify, the circle $C(g\tau, r)$ was replaced first by a square of the same center, of sides $2r$ parallel to the axes (Fig. 2), then by this same square rotated by 45° around its center. As
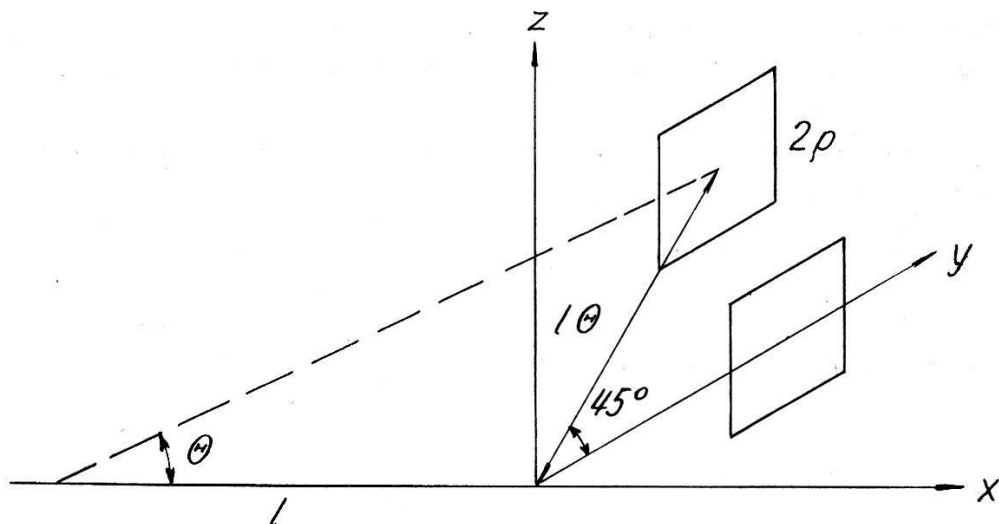

Fig. 2

shown in Table I, the results for the 2 domains of integration never differ by more than 6%. In Figure 3, the average of the 2 values of $\bar{g}$ has been plotted as a function of r.

Table 1

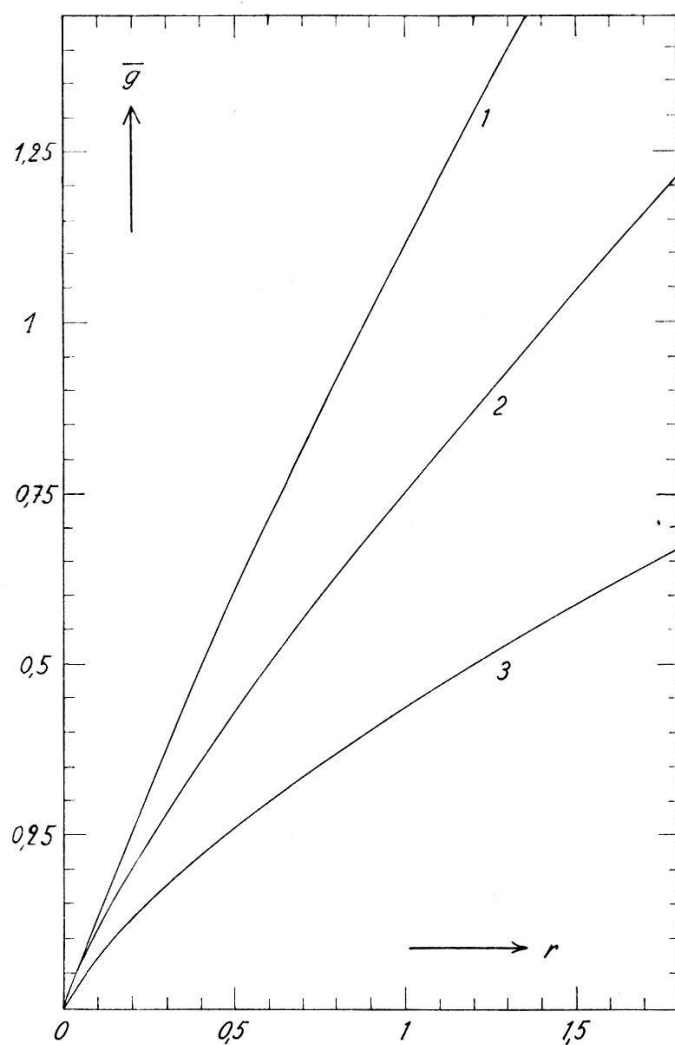| r	$\overline{g}_{//}$	$\overline{g}_{45°}$	$\overline{g}$
0·5	0·594	0·636	0·615
1·0	1·082	1·153	1·117
1·5	1·531	1·623	1·577
2·0	1·955	2·075	2·015
3·0	2·754	2·902	2·828
4·0	3·506	3·674	3·590
6·0	4·913	5·110	5·011
8·0	6·231	6·446	6·338
10·0	7·477	7·703	7·590
15·0	10·39	10·62	10·50
20·0	13·07	13·30	13·19
30·0	17·93	18·16	18·05
50·0	26·43	26·63	26·53
100·0	43·99	44·15	44·07
150·0	58·80	58·94	58·87
200·0	72·07	72·19	72·13
300·0	95·68	95·78	95·73

Fig. 3
This represents $\overline{g}$ as a function of r. The numbers on both scales have to be multiplied by 10 for curve 2, by 100 for curve 3. $\overline{g}$ and r are dimensionless quantities.

4. Evaluation of the number of pseudo-tridents

Coming back to the physical problem of determining the number of pseudo-tridents produced along the track of a particle, we have to take for ϱ a value depending on the radius of the track and such that a pair created within the distance ϱ cannot be distinguished from a direct pair. In photographic emulsions as well as in hydrogen diffusion chambers, the ratio ϱ/X_0 is about 10^{-5}. Since $\bar{g}$ is of the same order of magnitude as r (Fig. 3), one has

$$\frac{\bar{l}}{X_0} = \frac{(mc^2)^2}{D^2} \cdot \bar{g} \approx \frac{E-k}{mc^2} \cdot \frac{\varrho}{X_0} \approx 10^{-5} \cdot \frac{E-k}{mc^2}.$$

Therefore the hypothesis $l < X_0$ is verified for $E/mc^2 < 10^5$ *).

We still have to give the expression used for $\Sigma_p(k)$ in equation (3). Four different regions must be considered:

α) $2\, m_e\, c^2 < k < 20\, m_e\, c^2$: the contribution to the integral can be neglected, since pairs of energy lower than 10 MeV are hardly detectable because of their large opening angle.

β) $2\, m_e\, c^2 \ll k < 137\, m_e\, c^2 \cdot Z^{-1/3}$ (no screening): equation (9) page 81 of reference [4].

γ) $k \sim 137 \cdot m_e\, c^2 \cdot Z^{-1/3}$ (partial screening): Σ_p is given numerically by BETHE and HEITLER[8].

δ) $k \gg 137 \cdot m_e\, c^2 \cdot Z^{-1/3}$ (complete screening): equation (10) page 81 of reference [4].

In order to be able to integrate analytically, we have used the following expression for Σ_p:

$$\Sigma_p = \frac{1}{X_0 \ln(183\, Z^{-1/3})} \left(\frac{7}{9} \, ln \, \frac{2\,k}{m_e\, c^2} - \frac{109}{54} \right) \qquad \text{for } k \leqslant k_0 \text{ **)}$$

$$\Sigma_p = \frac{1}{X_0 \ln(183\, Z^{-1/3})} \left(\frac{7}{9} \left[ln\, (183\, Z^{-1/3}) - 2 \left(\frac{k_0}{k} \right)^{1/2} \right] - \frac{1}{54} \right) \quad \text{for } k \geqslant k_0$$

with

$$k_0 = \frac{1}{2}\, e^{\frac{4}{7}} \cdot 183\, Z^{-1/3} \cdot m_e\, c^2. \tag{7}$$

For the integration over k, $\bar{g}(r)$ is approximated by a linear function fitting the curve in the upper part of the domain of integration, this part giving the major contribution to the integral

$$\bar{g}(r) = \left[(1 + \varepsilon) \left(1 - \frac{k}{E} \right) + \zeta\, \frac{k}{E} \right] \bar{g}(r_{\text{max}}) \tag{8}$$

where

$$r_{\text{max}} = r\, (k = 0) = \frac{\varrho}{X_0} \cdot \frac{D^2 E}{(mc^2)^3}.$$

---

*) The number of pseudo-tridents produced by electrons in photographic emulsion has been calculated by TUMANYAN et al.[7] by a Monte Carlo Method, for few values of ϱ and for $E = 10^4$, 10^5 and 10^6 MeV.

**) This expression is obviously not valid for $k < 10\, m_e\, c^2$, but one can verify that its contribution to the integral (9) from 2 to 20 $m_e\, c^2$ cancels out almost exactly.

Taking (2), (4), (6) and (8) into account, equation (3) becomes

$$n_f = \int_k \sum_p(k) \left(\frac{m_e}{m}\right)^2 \frac{1}{X_0} \frac{dk}{k} \frac{(mc^2)^2}{D^2} X_0 \left[(1+\varepsilon)\left(1-\frac{k}{E}\right) + \right.$$

$$\left. + \zeta \frac{k}{E}\right] \bar{g}(r_{\max}) = \frac{(m_e c^2)^2}{D^2} \left[(1+\varepsilon)\int_{2 m_e c^2}^{E} \sum_p(k)\left(\frac{1}{k} - \frac{1}{E}\right) dk + \right.$$

$$\left. + \zeta \int_{2 m_e c^2}^{E} \sum_p(k)\frac{dk}{E}\right] \cdot \bar{g}(r_{\max}) =$$

$$= \frac{1}{X_0} \frac{(m_e c^2)^2}{D^2} \left[(1+\varepsilon) P(E, Z) + \zeta \cdot P_1(E, Z)\right] \bar{g}(r_{\max}) . \tag{9}$$

Introducing (7) and carrying out the integration yields for $E > k_0$:

$$\left. \begin{aligned} P(E, Z) &= \left(\frac{7}{9} - \frac{1}{54} \frac{1}{\ln(183\, Z^{-1/3})}\right) \ln \frac{E}{2\, m_e\, c^2} + \\[2mm] &+ \frac{1}{\ln(183\, Z^{-1/3})} \cdot \frac{28}{9} e^{\frac{2}{7}} \cdot (183\, Z^{-1/3})^{1/2} \left(\frac{2\, m_e\, c^2}{E}\right)^{1/2} - \\[2mm] &- \frac{1}{\ln(183\, Z^{-1/3})}\left(\frac{151}{54} - \frac{7}{9}\ln 4 + \frac{7}{36} e^{\frac{4}{7}} 183\, Z^{-1/3}\right)\frac{2\, m_e\, c^2}{E} - \\[2mm] &- \frac{7}{18}\ln(183\, Z^{-1/3}) - \left(\frac{1553}{378} - 2\ln 4 + \frac{7}{18}\ln^2 4\right)\frac{1}{\ln(183\, Z^{-1/3})} - \\[2mm] &- \frac{25}{9} + \frac{7}{9}\ln 4 . \end{aligned} \right\} \tag{10}$$

$$\left. \begin{aligned} P_1(E, Z) &= \frac{-1}{\ln(183\, Z^{-1/3})} \cdot \frac{14}{9} \cdot e^{\frac{2}{7}} \cdot (183\, Z^{-1/3})^{1/2} \cdot \left(\frac{2\, m_e\, c^2}{E}\right)^{1/2} + \\[2mm] &+ \frac{1}{\ln(183\, Z^{-1/3})}\left(\frac{151}{54} - \frac{7}{9}\ln 4 + \frac{7}{36} \cdot e^{\frac{4}{7}} \cdot 183\, Z^{-1/3}\right)\frac{2\, m_e\, c^2}{E} - \\[2mm] &- \frac{1}{\ln(183\, Z^{-1/3})} \cdot \frac{1}{54} + \frac{7}{9} . \end{aligned} \right\} \tag{11}$$

P and P_1 are plotted on Figure 4 as functions of E, for different values of Z. One can get a crude approximation of n_f by taking $\varepsilon = \zeta = 0$, or

$$n_f \cong \frac{1}{X_0} \frac{(m_e c^2)}{D^2} \cdot P(E, Z) \cdot \bar{g}(r_{\max}) . \tag{12}$$

For a better approximation, equation (9) should be used, with ε and ζ estimated from Figure (3). One sees easily from this Figure that $\varepsilon \approx 0 \cdot 02$ and $\zeta \approx 0 \cdot 1$ for most values of $r_{\max}$ (or E).

6. Applications

Consider for instance the case of 1 GeV electrons in photographic emulsion (Ilford G 5). We take the following values for the parameters of the medium: $\varrho = 0 \cdot 3\ \mu\text{m}$; $X_0 = 2 \cdot 99$ cm; $D = 11$ MeV*).

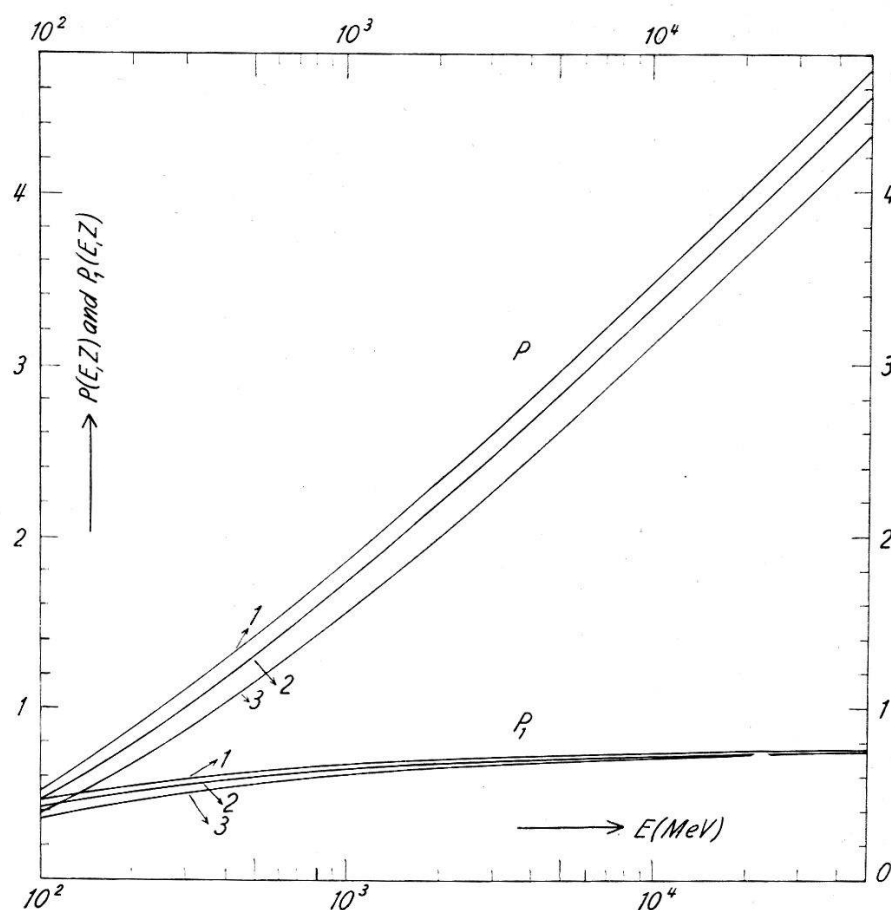*) This value has been determined experimentally for 380 MeV electrons.

Fig. 4   This figure represents P and P_1 as functions of E, for $Z = 82$ (curve 1), $Z = 13$ (curve 2), and $Z = 1$ (curve 3)

From Figure 3 and 4:

$$\bar{g}(r_{\max}) = 7{\cdot}05 \ (r_{\max} = 9{\cdot}1); \quad P = 1{\cdot}76; \quad P_1 = 0{\cdot}66;$$

admitting: $\varepsilon = 0$; $\zeta = 0{\cdot}12$, we have finally: $n_f = 9{\cdot}1 \cdot 10^{-3}$ pseudo-trident per cm.

This number is to be compared with the theoretical production rate of true tridents n_v. In Table 2, the ratio $n_f / n_f + n_v$ is given for various energies, n_v being calculated after BLOCK et al.[9]).

Table 2

E(MeV)	n_v (cm^{-1})		n_f (cm^{-1})		$\dfrac{n_f}{n_f + n_v}$
100	1·84	10^{-3}	0·35	10^{-3}	0·16
400	5·1	10^{-3}	2·9	10^{-3}	0·36
700	7·2	10^{-3}	5·9	10^{-3}	0·45
1000	8·8	10^{-3}	9·1	10^{-3}	0·51
1400	10·5	10^{-3}	13·2	10^{-3}	0·56
1700	11·5	10^{-3}	16·4	10^{-3}	0·59
2000	12·5	10^{-3}	20·0	10^{-3}	0·62

These results are correct at distances larger than 500 microns from the entrance in the emulsion (see § 2).

For μ-mesons of same velocity ($E/m_\mu c^2 = 2 \cdot 10^3$), r becomes $(m_e/m_\mu)^2$ times smaller, whereas the direct pair production cross-section remains unchanged. The proportion of pseudo-tridents is now completely negligible.

In a hydrogen diffusion chamber (pressure of 20 atmospheres), we have approximatively: $\varrho = 0\cdot01$ cm; $X_0 = 4 \cdot 10^4$ cm; $D = 11$ MeV.

For 1 GeV electrons, we find: $\bar{g}(r_{max}) = 0\cdot31$; ($r_{max} = 0\cdot24$); $P = 1,58$; and by the approximation (12): $n_f = 0\cdot28 \cdot 10^{-7}$ pseudo-trident per cm, to compare with $n_v = 2\cdot6 \cdot 10^{-7}$ direct pair per cm. In this case, the asymptotic value n_f is reached at about 30 cm from the walls.

The above computation can be applied to determine the radial distribution of the Bremsstrahlung pairs around the trajectory of the primary particle. In equation (9), only $\bar{g}$ depends on the radial distance ϱ; therefore the shape of the distribution is given by the derivative $d\bar{g}/dr$, which is approximately a constant (see Figure 3).

One can also apply this computation to the direct pair production by a charged particle in a thin target. A 'trident' is observed as a triplet of collimated tracks at the exit of the target. In this case, any pair produced in the target by a Bremsstrahlung photon constitutes a pseudo-trident. The total number of these events in a target of thickness $a \ll X_0$ is:

$$\left. \begin{aligned} N_p &= \int_{2 m_e c^2}^{E} dk \int_0^a dt\, (a - t) \sum_p(k) \sum_b(E, k) = \frac{a^2}{2} \int_{2 m_e c^2}^{E} dk \sum_p \sum_b = \\ &= \frac{a^2}{2} \frac{1}{X_0^2} \left(\frac{m_e}{m}\right)^2 [P(E, Z) + P_1(E, Z)] \end{aligned} \right\} \quad (13)$$

whereas the number of direct pairs is $N_v = a n_v$. With 1 GeV electrons in an aluminium target ($X_0 \cong 9$ cm), we have for instance $N_p/N_v = 0\cdot1$ for $a \cong 200$ μm.

Bibliography

[1]) M. BLOCK and D. T. KING, Phys. Rev. *95*, 171 (1954).
[2]) M. KOSHIBA and M. F. KAPLON, Phys. Rev. *97*, 193 (1955).
[3]) F. J. LOEFFLER, Phys. Rev. *108*, 1058 (1957).
[4]) B. ROSSI, High-Energy Particles, Prentice-Hall (1952).
[5]) R. WEILL, M. GAILLOUD and PH. ROSSELET, Nuovo Cimento *6*, 1430 (1957).
[6]) H. W. KOCH and J. W. MOTZ, Rev. Mod. Phys. *31*, 920 (1959).
[7]) V. A. TUMANYAN, V. A. ZHARKOV and G. S. STOLYAROVA, Dokl. Akad. Nauk SSSR. *122*, 208 (1958).
[8]) H. BETHE and W. HEITLER, Proc. Roy. Soc. *A 146*, 83 (1934).
[9]) M. M. BLOCK, D. T. KING and W. W. WADA, Phys. Rev. *96*, 1627 (1954).